Accepted Manuscript

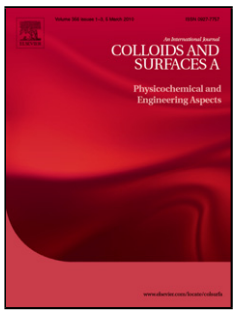

Title: NMR Cryoporometry of Polymers: Cross-linking, Porosity and the Importance of Probe Liquid

Authors: Taylor J. Rottreau, George E. Parkes, Manuela Schirru, Josephine L. Harries, Marta Granollers Mesa, Paul D. Topham, Rob Evans

PII: S0927-7757(19)30430-3
DOI: https://doi.org/10.1016/j.colsurfa.2019.05.018
Reference: COLSUA 23457

To appear in: *Colloids and Surfaces A: Physicochem. Eng. Aspects*

Received date: 28 January 2019
Revised date: 17 April 2019
Accepted date: 6 May 2019

Please cite this article as: Rottreau TJ, Parkes GE, Schirru M, Harries JL, Mesa MG, Topham PD, Evans R, NMR Cryoporometry of Polymers: Cross-linking, Porosity and the Importance of Probe Liquid, *Colloids and Surfaces A: Physicochemical and Engineering Aspects* (2019), https://doi.org/10.1016/j.colsurfa.2019.05.018

NMR Cryoporometry of Polymers: Cross-linking, Porosity and the Importance of Probe Liquid

Taylor J. Rottreau,[a] George E. Parkes,[a] Manuela Schirru,[a] Josephine L. Harries,[b] Marta Granollers Mesa,[a] Paul D. Topham[a] and Rob Evans[*a]*

[a]Aston Institute of Materials Research, School of Engineering and Applied Science, Aston University, Birmingham B4 7ET, United Kingdom.

[b]Domino Printing Sciences, Bar Hill, Cambridge, CB23 8TU, United Kingdom

[*]Corresponding author. Email address: r.evans2@aston.ac.uk. Telephone: 0121 204 5382

Abstract

The morphology of cross-linked polymers plays an important role in their physical and chemical properties. NMR cryoporometry allows for the investigation of these structures over different length scales, through appropriate choice of probe liquid. The different structures of two different polymeric samples, one a cross-linked polymer hydrogel, the other a pore-expanded ion-exchange polymer, are analysed here. The ability for NMR cryoporometry to analyse both polymeric materials in the swollen state is successfully demonstrated, as is the importance of probe-liquid choice for the analysis of different regions of the pore structure. In both cases, water is used to identify populations of pores smaller than *ca*. 5 nm. The use of

t-butanol and menthol reveals the presence of additional mesoporous structures in the ion-exchange resin as well as the responsiveness of the pore structure to the liquid used to swell it.

Keywords: nuclear magnetic resonance (NMR); cryoporometry; polymers, ion-exchange polymer; *t*-butanol; menthol;

Graphical abstract

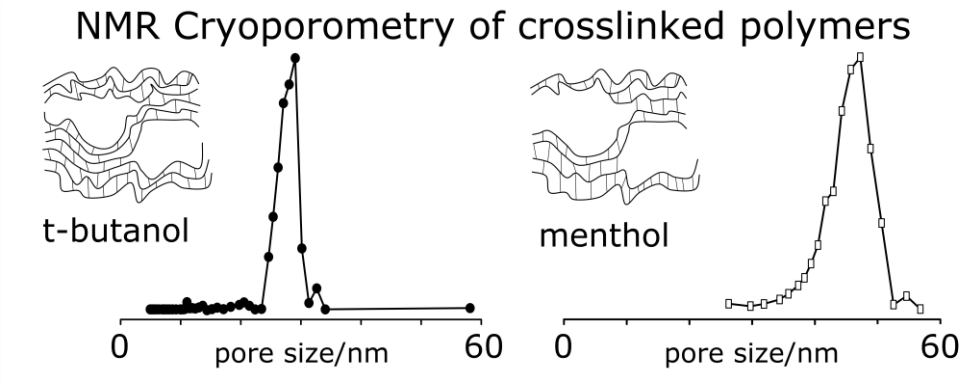

1. Introduction

Incorporating a three-dimensional cross-linked network to a polymer sample has a drastic effect on its structure and physical and chemical properties. Polymer hydrogels, for instance, typically have high water contents, large surface areas, and diverse fluctuating porosity [1-5]. These properties can render them extremely biocompatible [6] and they are commonly used for various applications including contact lenses [7], tissue engineering [8,9] and drug delivery [10]. The uses and applications of such materials depends on the both the pore structure and the state of any liquid, particularly water, within the cross-linked pore network. Nuclear magnetic resonance (NMR) cryoporometry [11-16] offers a robust and flexible method for obtaining such information about a range of different polymer networks.

There are a number of ways of describing and discussing the nature of water in porous gel systems. The porous system can be described in terms of the state of the water present within the network. In this context, there are three types of water present in polymer hydrogels. These are free water, which is present in the macropores, weakly-bound water, which may interact with the polymer, and strongly-bound or hydrogen-bonded water, which remains liquid below 258.15 K [17]. The pore structures themselves can also be described in terms of the pore sizes, where micro-, meso- and macropores are used to describe voids of $d < 2$ nm, $2 < d < 50$ nm and $d > 50$ nm, respectively [18]. The effective porosity and pore structures of these polymer systems is highly dependent on the amount of cross-linking present and also on the swelling of the polymer in, for example, aqueous solution. **Figure 1** is a schematic illustration of the typical changes in structure as the cross-linking percentage is increased. As the number of cross-linked polymer chains increases, so should the number of microporous structures in the material.

A separate class of cross-linked polymers are ion-exchange resins or, rather, ion-exchange polymers [19,20]. Based on water-insoluble polymers such as cross-linked polystyrene, subsequently functionalised, and typically synthesised in the form of micrometre-scale beads, the incorporation of polar groups onto the styrene groups means that these polymers can still exhibit swelling behaviour. Despite not necessarily containing macropores (i.e. pores greater than 50 nm in diameter), the cross-linked, net-like structure of ion-exchange polymers is often described as macroporous or macroreticular. Where they do differ from the more conventional gel-phase cross-linked polymers is in that they may have additional mesoporosity (i.e. pores between 2 and 50 nm in diameter) created by the addition of a porogen during the polymerisation process [21]. The porogen prevents further growth of the polymer chain and thus creates voids within the structure. The size of the void can be tailored by increasing or decreasing the amount of porogen used, albeit with the possibility of

structural frailties if too much porogen is added [22]. Examples of porogens include toluene, ethylbenzene and isobutanol [23]. As a result of this additional structure, macroreticular resins hold two main advantages over their gel-phase analogues; (1) they have an ordered porosity which can reach up to hundreds of nanometres in diameter, allowing larger species to travel through their architectures and (2) a higher cross-linking density can be achieved. Crucially, a higher cross-link density creates a more chemically stable system that is far more resistant to oxidation [23]. A schematic representation of the difference between a conventional cross-linked polymer gel and a macroreticular polymer is shown in **Figure 2**.

Macroreticular resins have proven to be effective catalysts, particularly in non-polar media where their lack of affinity for the reactants improves the separation of the desired products from the starting material [21]. Another major application of such resins is in water treatment [24]. Hard water contains ions such as calcium and magnesium and causes an undesirable build-up of scale in places including boiler systems. The resins soften the water by interchanging the divalent cations with sodium ions, followed by subsequent regeneration of the resin [21]. The choice of resin is tailored to remove different types of impurities contained in water. Four main types of ion-exchange polymers exist [25]; strongly acidic cation exchange (SAC), weakly acidic cation exchange (WAC), strongly basic anion exchange (SBA) and weakly basic anion exchange (WBA). In both example applications, the pore size and structure are important parameters to control in the optimisation of the application.

A number of methods exist for the measurement of pore sizes. Nitrogen porosimetry is a well-established technique for analysing polymeric materials in their dry state [26]. However, the materials studied here all find their applications when swollen with liquid. It is preferable to study their structures when in their operational state [27]. Differential scanning calorimetry (DSC) thermoporometry is a commonly used technique for analysing the

saturated porous structure of polymers. Weber *et al*. synthesized a series of ordered mesoporous poly(2-hydroxyethyl methacrylate-*co*-ethylene glycol dimethacrylate) networks employing the hard-templating methodology [28]. Analysis by DSC yielded pore sizes of 10-12 nm with little dependency on the cross-link density. The technique, however, has its limitations. Iza *et al*. revealed a significant variation in pore sizes when attempting to study the structure of poly[N-(2-hydroxypropyl) methacrylamide] (PHPMA) hydrogels in an aqueous solvent [29]. This variation was attributed to effects such as the heterogeneity of the structure and the cutting of the sample, as well as sensitivity issues with the technique.

NMR cryoporometry is an alternative thermoporometric approach. Whilst DSC is a transient heat flow technique, with a temperature sweep typically in the order of 0.1 to 1 K min^{-1}, the NMR method measures the melting/freezing processes in a series of discrete steps. NMR cryoporometry has been successfully demonstrated to work on a number of ordered polymeric matrices such as polymeric nanoparticles [30], porous polymer particles [31] and biodegradable polymer microparticles [32]. However, neither hydrogels nor swollen macroreticular resins have ever been studied using this technique.

Both DSC and NMR cryoporometry share the same basic principles, where an observed depression in melting point of a confined liquid is used to obtain a pore size distribution, as introduced by Gibbs and Thomson [33-38]. This melting point depression, ΔT_m, is predicted by Equation 1.

$$\Delta T_m = T_m - T_m(x) = \frac{4\gamma_{sl}T_m}{x\Delta H_f \rho_s} \quad (1)$$

where T_m is the bulk solid melting point, T_m (x) the melting point of a crystal with diameter x, γ_{sl} is the surface energy at the crystal-liquid interface, ΔH_f the bulk enthalpy of fusion, and ρ_s the density of the frozen probe liquid [39]. For any chosen liquid, the parameters in

Equation 1 can be collected into a single value, known as the melting point depression constant, k_c. This constant determines the range of pore sizes that a liquid can accurately analyze. An estimate for k_c can be obtained if values are known for the molar volume of the liquid, the free energy at the crystal/liquid interface, and the latent heat of melting. Invoking the additional contribution from a non-freezing surface layer, *l*, (labelled in other works variously as 2ε, $2sl$, ε, λ and τ) leads to Equation 2, which is used to determine the pore size given an experimentally acquired melting point depression.

$$\Delta T_m = \frac{k_c}{x-2l} \qquad (2)$$

Judicious selection of the probe liquid is paramount. The melting point of the liquid has to be accessible to the variable temperature apparatus of the spectrometer. The value of k_c is distinct for each liquid, and controls the range of pore sizes that can be accessed and analysed. Different values of k_c correspond to different ranges of pore sizes. If the pore is too large, then the melting point will not be depressed enough to be measured. On the other hand, if the molecule is too large, it simply cannot access the pores. A range of different liquids will be needed to explore the full range of length scales within the porous material. Solvent quality is a further, important, consideration here. The probe liquid needs to be able to access the porous structure. A good solvent will swell the polymer gel more than a theta, or a poor, one. The probe liquid may also influence the size of the pores it is measuring. In Amberlyst resins, the degree and extent of swelling observed is known to depend on the polarity of the solvent present.

In this work, NMR cryoporometry is used to analyse the porosity of two different polymer systems, a chemically cross-linked (disordered) copolymer hydrogel and an Amberlyst polymer resin. Both systems have extensive cross-linking with an effective

microporosity. The cross-link density was varied in the disordered hydrogel in order to assess the ability of NMR to quantify its density. In addition to this, Amberlyst has an ordered mesoporosity. To successfully measure and characterise these differences in pore sizes, architectures and chemistries requires probe liquids with different thermodynamic and physical properties. As such, four different probe liquids, water, *t*-butanol, menthol and cyclohexane, were chosen to illustrate the importance of matching the chemical, physical and thermodynamic parameters of the probe liquid to the material being analysed. The strong potential for NMR cryoporometry for the analysis of polymer pore structure is demonstrated, along with some cautionary notes about the importance of probe liquid choice.

2. Materials and Methods

2.1. HEA-HMAA

A general synthetic methodology for the poly(2-hydroxyethylacrylate-*co*-2-hydroxymethylacrylamide), P(HEA-*co*-HMAA), polymer hydrogels is supplied in SI.1.a. **Figure 3** shows the chemical structures of polymer and cross-linking groups.

2.2. Amberlyst A26 Resin

The resin was provided by the Dow Chemical Company. A general synthetic methodology is supplied in the SI.1.b. **Figure 3** shows the chemical structures of polymer and cross-linking groups.

2.3. NMR Experiments: Preparation

Menthol (Sigma-Aldrich, 99 %), *t*-butanol (Sigma-Aldrich, 99 %), cyclohexane (Fisher Scientific, 99 %) and DI water were used without additional purification. A small amount of

each polymer (*ca*. 20 mg) was initially placed in a sample tube prior to the addition of the solvent. The polymer was allowed to swell in the solvent for approximately 24 hours to ensure that the equilibrium solvent content was attained; confirmed by excess residual liquid remaining in the vial. The polymer was then carefully removed from the liquid and blotted in pre-soaked filter paper to remove any excess. The sample was transferred to a 5 mm standard NMR tube and sealed with parafilm. The samples containing *t*-butanol and menthol were kept above their corresponding bulk melting temperatures to prevent early freezing of the probe liquid.

2.4. NMR Experiments: Cryoporometry

All NMR measurements were carried out on a Bruker Avance spectrometer, equipped with a 5 mm PABBO BB-1H Z-GRD probe, with a frequency of 300 MHz.

To obtain suitably low temperatures, a Bruker BVT3200 temperature control system, with a stated precision of 0.1 K, was used. The cooling system passes a combination of N_2 gas and air over the sample at a flow rate of 400 l h^{-1} with the probe heater set to a maximum of 17% output. Before starting experimental work, the temperature control system was calibrated using a deuterated methanol NMR thermometer, producing a calibration relationship between the nominal spectrometer temperature and actual sample temperature [38]. For all cryoporometric studies, the probe was tuned and matched at all temperatures except those close to the expected phase transitions of the liquid to ensure any changes to the signal intensity during this period were a result of the phase change only.

NMR spectra of the polymer/liquid samples were acquired with the CPMG [41,42] pulse sequence using a total echo time of 4 ms for all experiments. The CPMG spin-echo was used to ensure that broad signals of the polymers were removed in all experiments. Typical sets of 1H NMR spectra detailing melting curves, with complete removal of any background

polymer signals, are included in the SI. To acquire an NMR melting curve, such as in SI.2, the temperature was initially decreased until no signal was observed *i.e*. when the sample was completely frozen. The temperature was then increased in steps of 0.2-0.3 K. At each temperature step, before the acquisition of NMR data, the sample was left to equilibrate for at least 10 minutes from when the NMR signal stopped changing in intensity. Acquired NMR signal intensities have been corrected to account for the effect of Curie's law, where the signal intensity decreases with increasing temperature outside of phase transformations [43]. The signal intensities are then further normalized to a value where all of the confined water is liquid and any negligible remaining amount of bulk water remains frozen.

2.5. Differential Scanning Calorimetry

The DSC measurements were made using a Mettler-Toledo DSC 1 STAR^e system equipped with a liquid nitrogen cooling supply. Samples of approximately 2 mg of the water swollen P(HEA-*co*-HMAA) polymer were used. The samples were initially taken down to 228 K to ensure all of the liquid was frozen. A heating rate of 0.5 K min^{-1} was used through to a final temperature of 283 K. To transform the DSC melting curves into a pore size distribution, the procedure outlined in Majda *et al*. was followed [44].

2.6. SEM Imaging

SEM images of the 25% cross-linked P(HEA-*co*-HMAA) polymer were obtained from TESCAN using a JSM-7200F Field Emission SEM. For sample analysis, lower acceleration voltages of approximately 1-2 kV and a detection system, including chamber-SE and in-beam SE detectors, were used.

3. Results and Discussion

3.1. P(HEA-*co*-HMAA): Water as a Probe Liquid

Figure 4 follows the melting of water in four P(HEA-*co*-HMAA) polymer samples, with varying cross-link densities. In all samples, the NMR signal intensity increases with temperature, as the water confined within the cross-linking networks melts. No further rise is observed past the bulk melting temperature suggesting that no water was present on the exterior of the gels. As the cross-linking percentage is increased, the density of smaller effective pores also increases. This behaviour is revealed in **Figure 4**, where there is a proportion of water, present within these smaller pores, that melts at a lower temperature. This is revealed by the increase in signal intensity at lower temperatures, most visible in the melting curve data of the 25% cross-linked sample. As the temperature is increased closer to that of bulk melting, it tends towards that of the other three samples.

In order to convert the melting point data to a pore size distribution, parameters from reference 39 were used where water was estimated to have a melting point depression constant of 49.53 K nm and a non-freezing surface layer of 0.53 nm [45]. **Figure 5** shows the conversion of the melting point data (**Figure 4**) into pore size distributions lower than 5 nm. As a probe liquid in cryoporometry experiments, water is much more suited to analysing structures which have small pores, a reflection of its melting point depression parameters.

Figure 5 reveals a correlation between the percentage of cross-linking in the polymer sample and the population of weakly-bound water present, as shown by the increase in relative pore volume for up to 5 nm. The pore size distributions indicate that a larger volume of water is present in the mesoporous region of the 25% cross-linked polymer, confirming the

hypothesis that the polymer has an increased amount of smaller effective pores compared to the other samples as a result of the higher cross-link density. Similarly, the 1.25% cross-linked polymer contained the least amount of water in this region, reflecting lower density of effective pores smaller than 5 nm in size. Outside of this region, however, the relative pore volume for water continuously increases with no plateau prior to the bulk melting region – illustrating the extent of swelling of the polymer in water and the presence of a large concentration of free water. The results demonstrate the ability of NMR cryoporometry, using water as the probe liquid, to distinguish differences in cross-linking density in a disordered polymer hydrogel.

3.2. P(HEA-*co*-HMAA): Application of Other Probe Liquids

Further NMR cryoporometric experiments were attempted, using *t*-butanol, menthol and cyclohexane as probe liquids. No pore melting was observed for any of the three liquids. Before cross-linking, the polymer was soluble in both water and *t*-butanol but insoluble in menthol and cyclohexane. The cross-linked polymer was insoluble in all four liquids. In spite of its favourable polarity, *t*-butanol did not cause the polymer to swell significantly enough to enter the microporous structure of the cross-linked polymer. The failure to reproduce measurements of the smallest pore sizes (those depicted in **Figure 5**) using *t*-butanol are shown in SI.3. There is no evidence of any mesoporosity or bound probe liquid. Similar results were obtained using both menthol, despite a polar hydroxyl group present in the molecule, and cyclohexane, as both probe liquids are unfavourable solvents for the original polymer.

3.3. P(HEA-*co*-HMAA): Confirmation with Microscopy

To further characterise the polymer, SEM images were obtained for the 25% cross-linked polymer swollen in water. **Figure 6** contains a series of four SEM images between 10 and 1

μm in scale. A further set of images at lower magnifications are included in SI.4. These images reveal structural information about the polymer matrix, including the possible identification of polymer fibres, the presence of macropores and also the presence of a nanometre scaled fine structure. The cross-linking creates large voids, approximately 2-3 μm in diameter. These pore sizes are far too big to depress a liquid melting point enough to be observed by either NMR or DSC analyses. It is in the finer structure of the polymer, most visible in **Figure 6(d)**, where the effective microporosity, consistent with the NMR melting data and pore size distributions of **Figures 4** and **5**, may be present.

3.4. P(HEA-*co*-HMAA): Confirmation with DSC measurements

DSC was unable to provide any quantitative information on the effective porosity of the gel. As illustrated in SI.5, even at the lower end of possible pore sizes, DSC was unable to detect the same pore melting that NMR recorded. No observable melting, let alone observable differences in water behaviour across the cross-linked series, was observed for this set of polymer materials. As such, NMR boasts some advantages over DSC, even though both fail to quantitatively deduce the nature of water throughout the swollen polymer.

3.5. Amberlyst: Water as a Probe Liquid

In contrast to the P(HEA-*co*-HMAA) polymer hydrogel, the Amberlyst resin has porosity on two different length scales. It is the microporosity, caused purely by the cross-linking, that defines how well the Amberlyst can swell in solution. Macroreticular resins, especially those with a low cross-link density, remain collapsed [46], or only swell slightly, in nonpolar solvents [47]. The second, mesoporous, region of porosity is highly ordered. This region is readily accessible for analysis using NMR cryoporometry.

The resin was first analysed using water as the swelling liquid. **Figure 7(a)** shows the melting of water confined within the polymer matrix. The absence of a plateau in signal

intensity with respect to temperature, similar to that observed with all four P(HEA-*co*-HMAA) samples in **Figure 4**, suggests that the polymer swells significantly in water, with a large proportion of free water present. Free water remains unaffected by the polymer network. Strongly bound water is simply not observable by the NMR method, as it does not freeze at the temperatures achieved by the experimental method. A small concentration of weakly bound water is confirmed to exist, corresponding to a microporous region in the material. A pore size distribution (**Figure 7(b)**), obtained using the melting point depression parameters used previously with P(HEA-*co*-HMMA), indicates a small proportion of water in a weakly bound state, similar to that found in the hydrogel previously, but most of the water content is in pores too large to depress the melting point enough to be observed. These results suggest an inability of NMR cryoporometry to measure an accurate pore size using water as the probe liquid in this polymer system. The swelling of the polymer, and the added macroreticular structure, leads to the substantial presence of free water and effective pore sizes too large for thermoporometry analysis.

3.6. Amberlyst: Other Probe Liquids

To probe the macroreticular structure of the resin, the polymer was saturated in *t*-butanol and also in menthol. These alcohols have been demonstrated to work reliably in NMR cryoporometry measurements of controlled pore glasses [48]. NMR was able to detect confined melting for *t*-butanol in the mesopores of Amberlyst A26OH. **Figure 8(a)** follows the melting transition from completely frozen through to complete pore melting. The melting curve data was converted into a pore size distribution (**Figure 8(b)**), using melting point depression parameters from reference 48 (k_c = 119.2 K nm and 2*l* = 1.7 nm [48]) and an average pore diameter of 29 nm was obtained. This is in excellent agreement with the average pore diameter reported by the manufacturer in the dry state, and also that obtained by

combined nitrogen and mercury porosimetry [49]. This implies that very little swelling of the mesoporous region occurs when the resin is swelled with *t*-butanol.

Figure 9(a) depicts the NMR melting curve of menthol within the pores of the resin, data converted to a pore size distribution in **Figure 9(b)**, again using melting point depression parameters from reference 48 (k_c = 219.3 K nm and 2*l* = 1.9 nm [48]).

The pore size distribution reveals an average pore diameter of 47 nm. This is significantly larger than the pore diameter obtained using *t*-butanol as the probe liquid. The differences here can be attributed to the different swelling behaviour of the ion exchange polymer in the presence of different liquids, with different polarities and different interactions between the liquids and both the polymer backbone and the functional groups. The added mesopores are known to swell to different extents depending on the nature of the liquid present. Additionally, no pore melting was observed for cyclohexane. Cyclohexane may simply be too hydrophobic to swell the polymer.

4. Conclusions

This is the first time that NMR cryoporometry has been used to accurately determine pore sizes for a macroreticular resin in the swollen state. The Amberlyst resin used in this work contains ordered regions of mesoporosity, created by the addition of a porogen during the polymerisation process. Pore size distributions corresponding to this mesoporosity were successfully obtained using both *t*-butanol and menthol. It has been shown in a number of previous studies that the ordered mesopore structure of macroreticular resins can change, depending on the polarity of the liquid to which it is subjected to [46,47, 50]. NMR

cryoporometry reveals this behaviour. Note that, it would not be at all possible to explore these phenomena using gas techniques.

While menthol is only slightly larger than *t*-butanol, the pores expand to almost twice the size of those observed in the presence of the smaller alcohol. As the swelling behaviour of a macroreticular polymer is a function of the interactions of the solvent with both the polymer backbones and with any functional groups present, the dependence of swelling on the liquid used is not trivial. For example, the resins in Reference 49 that are most similar to Amberlyst A26 (*i.e*. cross-linked polystyrene polymers containing basic quaternary ammonium groups) showed an increase in swelling in ethanol compared to water, but small differences in the basicity of the resins lead to strong differences in the swelling behaviour when in benzene.

In comparison to the other, widely used, thermoporometric technique, DSC, NMR holds some advantages. DSC calibration methods have not yet been obtained for alcohols such as *t*-butanol and menthol in order to convert the heat flow data into a pore size distribution. However, melting point depression data for any liquid can be used to estimate values for k_c and 2*l* [51, 52]. There are also further complications in preparation of the sample, due to the relatively high bulk melting point of menthol, which can be controlled easier during the sample preparation process when the sample is in an NMR tube, compared to a DSC crucible. NMR cryoporometry also allows for the acquisition of both melting and freezing curves, which can reveal valuable information about the geometry and structure of the pores, such as bottlenecks and 'inkwell' structures [53].

The analysis of the P(HEA-*co*-HMAA) polymer suggests that cryoporometry may have some limitations when trying to analyse a microporous polymer gel system. The polymer swelled significantly when subjected to water which suggested, at first instance, that no porosity data, qualitatively or quantitatively, could be obtained. However, by focusing on the

region that has previously proven to be most effective for water (<10 nm), differences between samples with different cross-linking percentages become clear. A larger proportion of weakly bound water was found in the polymer sample with the highest amount of cross-linking due to the higher density of smaller micropores formed. However, the polymer failed to swell in the other three liquids. This may be due to two reasons. First, there is a mismatch of chemical properties. While menthol contains a polar group, cyclohexane is apolar, and the original polymer, before cross-linking, does not dissolve in either liquid. As such, the hydrogel pores remain collapsed in the presence of cyclohexane and menthol. Second, the molecular sizes of cyclohexane, menthol and *t*-butanol are all significantly larger than that of water (see SI.7 for estimations of molecular size for all four probe liquids). Note that cyclohexane and *t*-butanol are similar in molecular size but differ in polarity, with the original polymer dissolving in the tertiary alcohol. However, a combination of the increased molecular size of *t*-butanol compared with water and the increased rigidity of the polymer backbone introduced by the cross-linking reaction suggest that, while smaller than the pore sizes measured, the alcohol may simply be too large to cause the cross-linked polymer to swell.

This work demonstrates that NMR cryoporometry can be used to study the pore structures and dimensions of different polymeric systems. Importantly, the probe liquid needs to be matched to the properties of the polymer, not only in terms of chemistry but also in terms of the sizes of the pores being studied and the probe liquids used to study them. Where mesoporous structures exist, as in macroreticular resins, pore sizes can be responsive to the nature of the swelling liquid. Ion exchange polymers are key to many areas of science and their proficiency lies in the fact that their properties change in the swollen state. NMR cryoporometry can measure these changes and, more generally, offers the ability to

accurately probe mesoporous structures in their operational, wet, state in order to elucidate important structural information.

Acknowledgments

Financial support for Ph.D. studentships for TJR and MS from the School of Engineering and Applied Science, Aston University, is gratefully acknowledged. The authors would also like to thank DowDuPont for supplying the macroreticular ion exchange resin. To access the research data supporting this publication, please see: https://data.mendeley.com/datasets/gfch82kgm4/1.

References

[1] A. S. Hoffman, in *Polym. Med. Surg.*, Springer US, New York, 1975, pp. 33-44.

[2] K. Wang, J. Burban and E. Cussler, in *Responsive Gels*, Springer, Berlin Heidelberg, 1993, pp. 67-79.

[3] O. Wichterle and D. Lim, Hydrophilic Gels for Biological Use, *Nature*, 1960, 185, 117-118.

[4] J. Chen, W. E. Blevins, H. Park and K. Park, Gastric retention properties of superporous hydrogel composites, *J. Control. Release*. 2000, 64, 39-51.

[5] D. G. Pedley, P. J. Skelly and B. J. Tighe, Hydrogels in Biomedical Applications, *British Polymer Journal*, 1980, 12, 99-110.

[6] E. H. Schacht, Polymer chemistry and hydrogel systems, *J. Phys.: Conf. Ser.*, 2004, 3, 22-28.

[7] P. C. Nicolson and J. Vogt, Soft contact lens polymers: an evolution, *Biomaterials*, 2001, 22, 3273-3283.

[8] K. Y. Lee and D. J. Mooney, Hydrogels for tissue engineering, *Chem. Rev.*, 2001, 101, 1869-1879.

[9] J. L. Drury and D. J. Mooney, Hydrogels for tissue engineering: scaffold design variables and applications, *Biomaterials*, 2003, 24, 4337-4351.

[10] T. R. Hoare and D. S. Kohane, Hydrogels in drug delivery: Progress and challenges, *Polymer*, 2008, 49, 1993-2007.

[11] J. Mitchell, J. B. W. Webber and J. H. Strange, Nuclear Magnetic Resonance Cryoporometry, *Phys. Rep.* 2008, 461, 1-36.

[12] O. V. Petrov and I. Furó, NMR cryoporometry: Principles, applications and potential, *Prog. Nucl. Magn. Reson. Spectrosc*. 2009, 54, 97-122.

[13] J. B. W. Webber, R. Anderson, J. H. Strange and B. Tohidi, Clathrate formation and dissociation in vapour/water/ice/hydrate systems in SBA-15, Sol-Gel and CPG porous media, as probed by NMR relaxation, novel protocol NMR Cryoporometry, Neutron Scattering and ab-initio QM-MD simulation, *Magn. Reson. Imaging*, 2007, 25, 533-536.

[14] S. Jähnert, F. Vaca Chávez, G. E. Schaumann, A. Schreiber, M. Schönhoff and G. H. Findenegg, Melting and freezing of water in cylindrical silica nanopores, *Phys. Chem. Chem. Phys*., 2008, 10, 6039-6051.

[15] O. V. Petrov and I. Furó, A study of freezing–melting hysteresis of water in different porous materials. Part II: surfactant-templated silicas, *Phys. Chem. Chem. Phys*., 2011, 13, 16358-16365.

[16] N. Buchtová, A. D'Orlando, P. Judeinstein, O. Chauvet, P. Weiss and J. Le Bideau, Water dynamics in silanized hydroxypropyl methylcellulose based hydrogels designed for tissue engineering, *Carbohydr. Polym*., 2018, 202, 404-408.

[17] I. N. Savina, V. M. Gun'ko, V. V. Turov, M. Dainiak, G. J. Phillips, I. Y. Galaev and S. V. Mikhalovsky, Porous structure and water state in cross-linked polymer and protein cryo-hydrogels, *Soft Matter*, 2011, 7, 4276-4283.

[18] R. K. Harris, J. Kowalewski and S. C. de Menezes, International Union of Pure and Applied Chemistry Physical Chemistry Division Commission on Molecular Structure and Spectroscopy. Parameters and symbols for use in nuclear magnetic resonance (IUPAC recommendations 1997), *Magn. Reson. Chem*., 1998, 36, 145-149.

[19] K. Horie, M. Barón, R. B. Fox, J. He, M. Hess, J. Kahovec, T. Kitayama, P. Kubisa, E. Maréchal, W. Mormann, R. F. T. Stepto, D. Tabak, J. Vohlídal, E. S. Wilks and W. J. Work, Definitions of terms relating to reactions of polymers and to functional polymeric materials (IUPAC Recommendations 2003), *Pure Appl. Chem*., 2004, 76, 889-906.

[20] R. Kunin, E. Meitzner and N. Bortnick, Macroreticular Ion Exchange Resins, *J. Am. Chem. Soc*., 1962, 84, 305-306.

[21] R. Kunin and R. L. Gustafson, Ion Exchange, *Ind. Eng. Chem. Res*., 1969, 61, 38-42.

[22] A. G. Lee, C. P. Arena, D. J. Beebe and S. P. Palecek, Development of macroporous poly(ethylene glycol) hydrogel arrays within microfluidic channels, *Biomacromolecules*, 2010, 11, 3316-3324.

[23] I. M. Abrams and J. R. Millar, A history of the origin and development of macroporous ion-exchange resins, *React. Funct. Polym*., 1997, 35, 7-22.

[24] J. C. Crittenden, R. R. Trussell, D. W. Hand, K. J. Howe and G. Tchobanoglous, in *MWH's Water Treatment: Principles and Design*, Third Edition, Wiley-VCH, Weinheim, 2012.

[25] F. de Dardel and T. V. Arden in *Ullmann's Encyclopedia of Industrial Chemistry*, Wiley-VCH, Weinheim, 2002.

[26] S. Gregg and K. Sing, *Adsorption, Surface Area and Porosity*, Academic Press, London, 1967.

[27] B. Corain, M. Zecca and K. Jeřábek, Catalysis and polymer networks — the role of morphology and molecular accessibility, *J. Mol. Catal.*, 2001, 177, 3-20.

[28] J. Weber and L. Bergstrom, Mesoporous Hydrogels: Revealing Reversible Porosity by Cryoporometry, X-ray Scattering, and Gas Adsorption, *Langmuir*, 2010, 26, 10158-10164.

[29] M. Iza, S. Woerly, C. Danumah, S. LKaliaguine and M. Bousmina, Determination of pore size distribution for mesoporous materials and polymeric gels by means of DSC measurements: thermoporometry, *Polymer*, 2000, 41, 5885-5893.

[30] N. Gopinathan, B. Yang, J. P. Lowe, K. J. Edler and S. P. Rigby, NMR cryoporometry characterisation studies of the relation between drug release profile and pore structural evolution of polymeric nanoparticles, *Int. J. Pharm.*, 2014, 469, 146-158.

[31] E. W. Hansen, G. Fonnum and E. Weng, Pore Morphology of Porous Polymer Particles Probed by NMR Relaxometry and NMR Cryoporometry, *J. Phys. Chem. B*, 2005, 109, 24295-24303.

[32] O. Petrov, I. Furo, M. Schuleit, R. Domanig, M. Plunkett and J. Daicic, Pore size distributions of biodegradable polymer microparticles in aqueous environments measured by NMR cryoporometry, *Int. J. Pharm.*, 2006, 309, 157-162.

[33] J. W. Gibbs, *The Collected Works of J. Willard Gibbs*, Longmans, Green & Co, London, 1928.

[34] J. W. Gibbs, *The Scientific Papers of J. Willard Gibbs*, New Dover Edition, Longmans, Green & Co, London, 1906.

[35] J. Thomson, Theoretical Considerations on the Effect of Pressure in Lowering the Freezing Point of Water, *Trans. Roy. Soc.*, 1849, 5, 575-580.

[36] J. Thomson, On crystallization and liquefaction, as influenced by stresses tending to change of form in the crystals, *Proc. Roy. Soc.*, 1862, 11, 473-481.

[37] J. J. Thomson, *Applications of Dynamics to Physics and Chemistry*, Macmillan & Co, London, 1888.

[38] W. Thomson, On the equilibrium of vapour at a curved surface of liquid, *Phil. Mag. Series.*, 1871, 42, 452-488.

[39] C. L. Jackson and G. B. Mckenna, The melting behavior of organic materials confined in porous solids, *J. Chem. Phys.*, 1990, 93, 9002-9011.

[40] M. Findeisen, T. Brand and S. Berger, A ^{1}H-NMR thermometer suitable for cryoprobes. *Magn. Reson. Chem.*, 2007, 45, 175-178.

[41] H. Y. Carr and E. M. Purcell, Effects of Diffusion on Free Precession in Nuclear Magnetic Resonance Experiments, *Phys. Rev.*, 1954, 94, 630-638.

[42] S. Meiboom and D. Gill, Modified Spin- Echo Method for Measuring Nuclear Relaxation Times, *Rev. Sci. Instrum.*, 1958, 29, 688-691.

[43] A. Abragam, *The Principles of Nuclear Magnetism*, Clarendon Press, Oxford, 1961.

[44] D. Majda, W. Makowski and M. Manko, Pore size distribution of micelle-templated silicas studied by thermoporosimetry using water and n-heptane, *J. Therm. Anal. Calorim.*, 2012, 109, 663-669.

[45] T. J. Rottreau, C. M. A. Parlett, A. F. Lee and R. Evans, NMR cryoporometric measurements of porous silica: A method for the determination of melting point depression parameters of probe liquids, *Microporous Mesoporous Mater.*, 2018, 264, 265-271.

[46] M. Granollers, J. F. Izquierdo and F. Cunill, Effect of macroreticular acidic ion-exchange resins on 2-methyl-1-butene and 2-methyl-2-butene mixture oligomerization, *Appl. Catal., A.*, 2012, 435-436, 163-171.

[47] A. Golloch, *Handbook of Rare Earth Elements: Analytics*, Walter de Gruyter GmbH & Co KG, 2017.

[48] T. J. Rottreau, C. M. A. Parlett, A. F. Lee and R. Evans, Extending the range of liquids available for NMR cryoporometry studies of porous materials, *Microporous Mesoporous Mater.*, 2019, 274, 198-202.

[49] K. A. Kun and R. Kunin, The Pore Structure of Macroreticular Ion Exchange Resins, *J. Polym. Sci.*, 1967, C16, 1457-1469.

[50] G. W. Bodamer and R. Kunin, Behavior of Ion Exchange Resins in Solvents Other Than Water: Swelling and Exchange Characteristics, *Ind. Eng. Chem.*, 1953, 45, 2577-2580.

[51] H. K. Christenson, Confinement effects on freezing and melting, *J. Phys. Condens. Matter*, 2001, 13, R95–R133.

[52] Y. Qiao and H.K. Christenson, Triple-Point Wetting and Liquid Condensation in a Slit Pore, Phys. Rev. Lett., 2001, 86, 3807–3810.

[53] I. Hitchcock, E. M. Holt, J. P. Lowe and S. P. Rigby, Studies of freezing-melting hysteresis in cryoporometry scanning loop experiments using NMR diffusometry and relaxometry, *Chem. Eng. Sci.*, 2011, 66, 582-592.

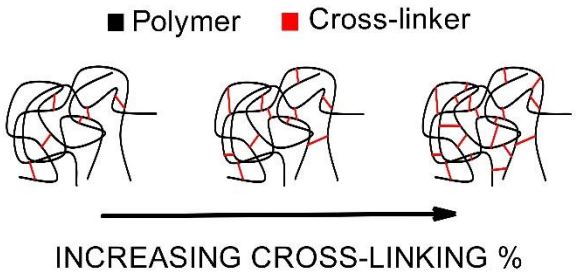

Figure 1. Schematic illustration of increasing percentage of cross-linking within the polymer network.

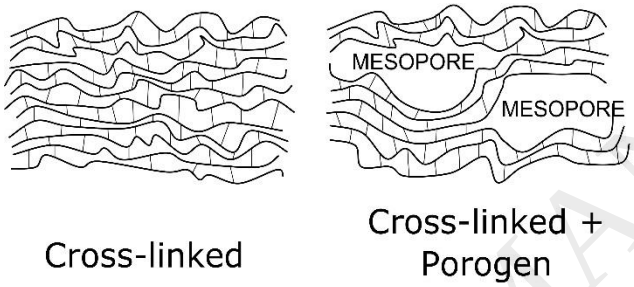

Figure 2. Schematic representation of the structural difference between a cross-linked polymer gel and a macroreticular ion exchange polymer.

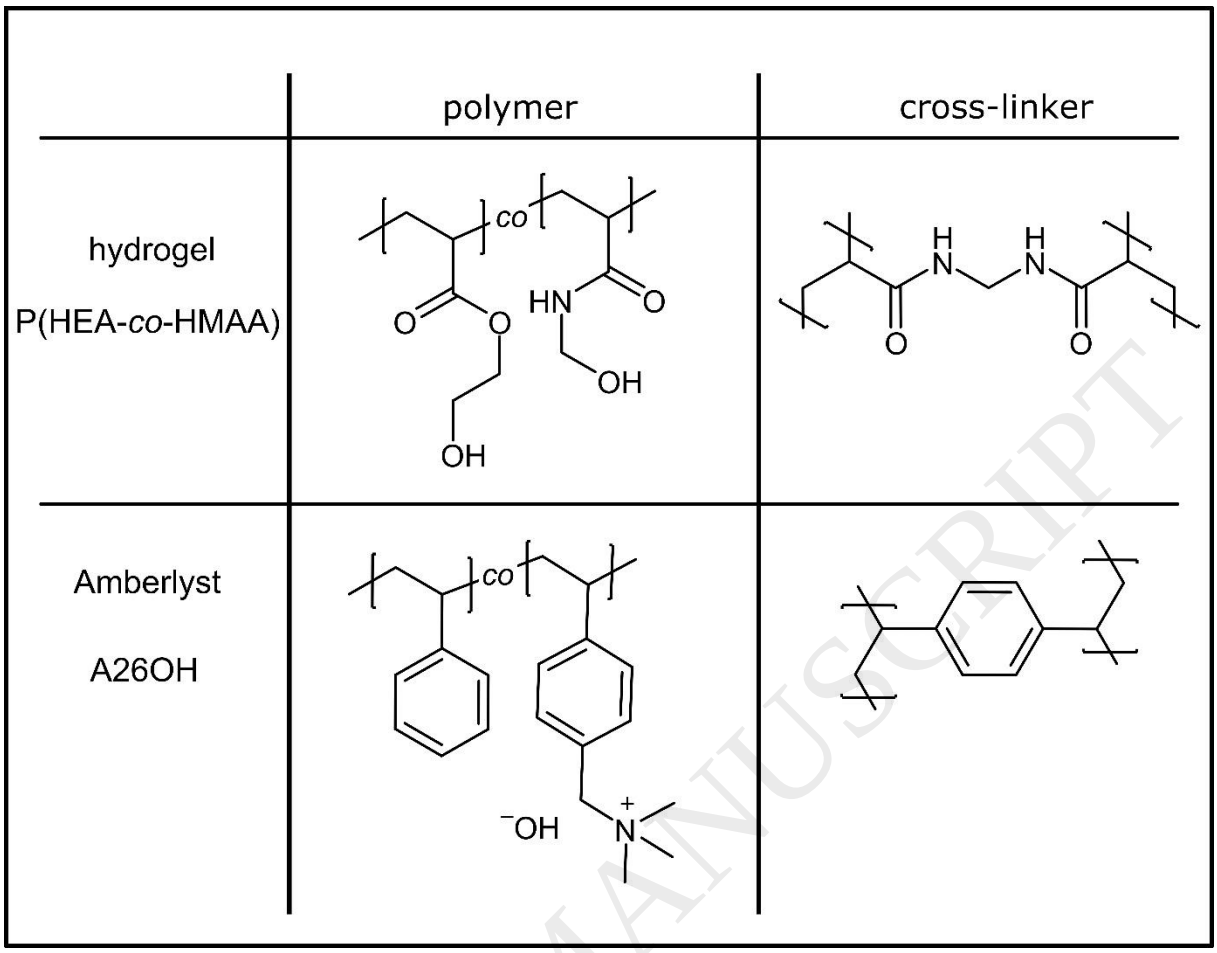

Figure 3: Summary of polymer and cross-linker chemical structures for the two polymer systems used in this study.

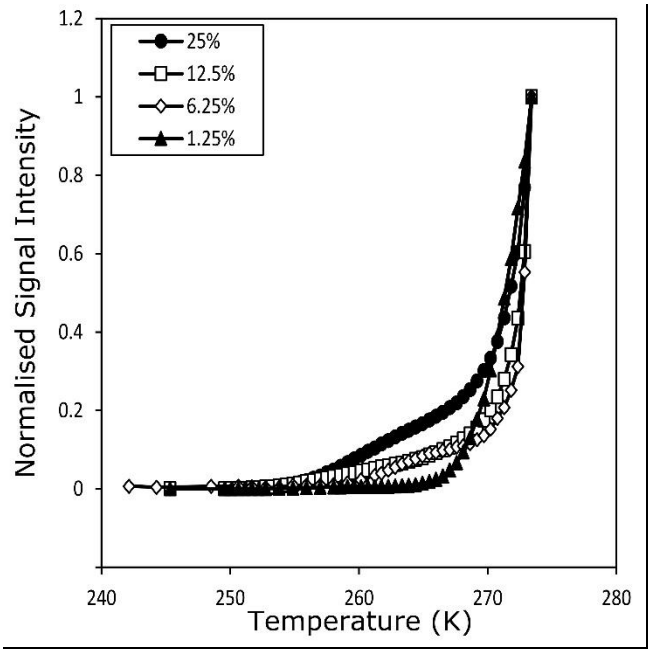

Figure 4. NMR melting curves for the water-swollen P(HEA-*co*-HMAA) polymer samples containing 25 % (filled circle), 12.5 % (hollow square), 6.25 % (hollow diamond) and 1.25 % (filled triangle) cross-linker.

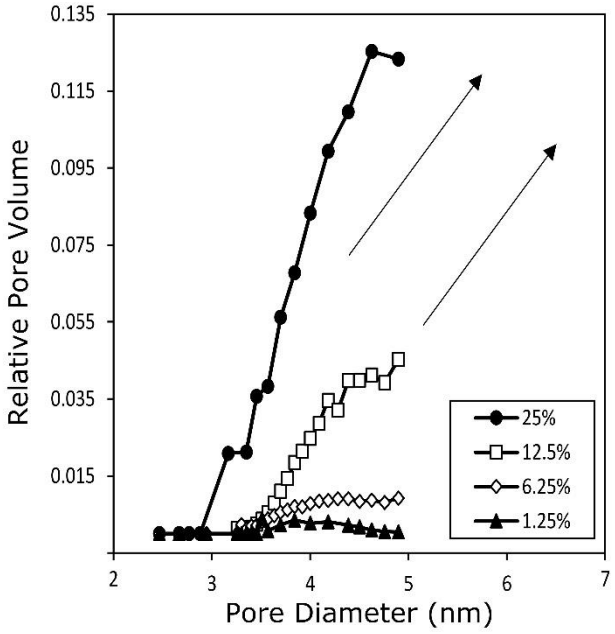

Figure 5. Pore size distribution data obtained from melting water confined in the pores of the P(HEA-*co*-HMAA) polymer samples containing 25 % (filled circle), 12.5 % (hollow square), 6.25 % (hollow diamond) and 1.25 % (filled triangle) cross-linker, calculated for pores lower than 5 nm in size.

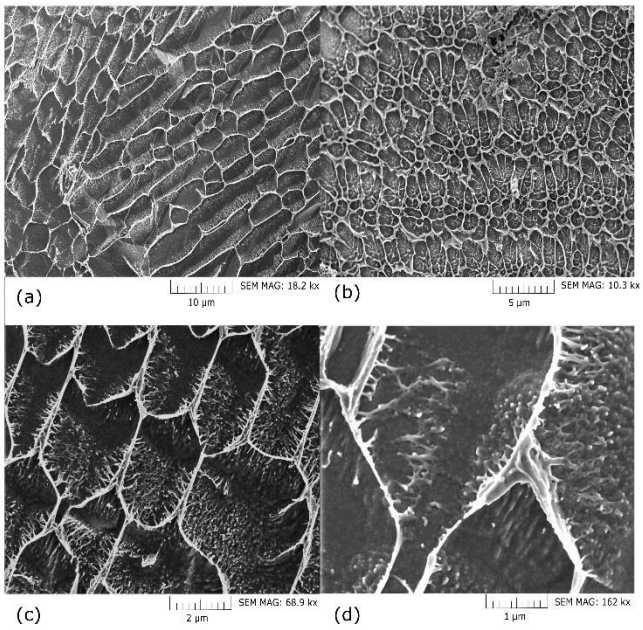

Figure 6. SEM images of the water-swollen P(HEA-*co*-HMAA) polymer, with 25% cross-linker, at magnifications of (a) 18.2k ×, (b) 10.3k ×, (c) 68.9k × and (d) 162k ×.

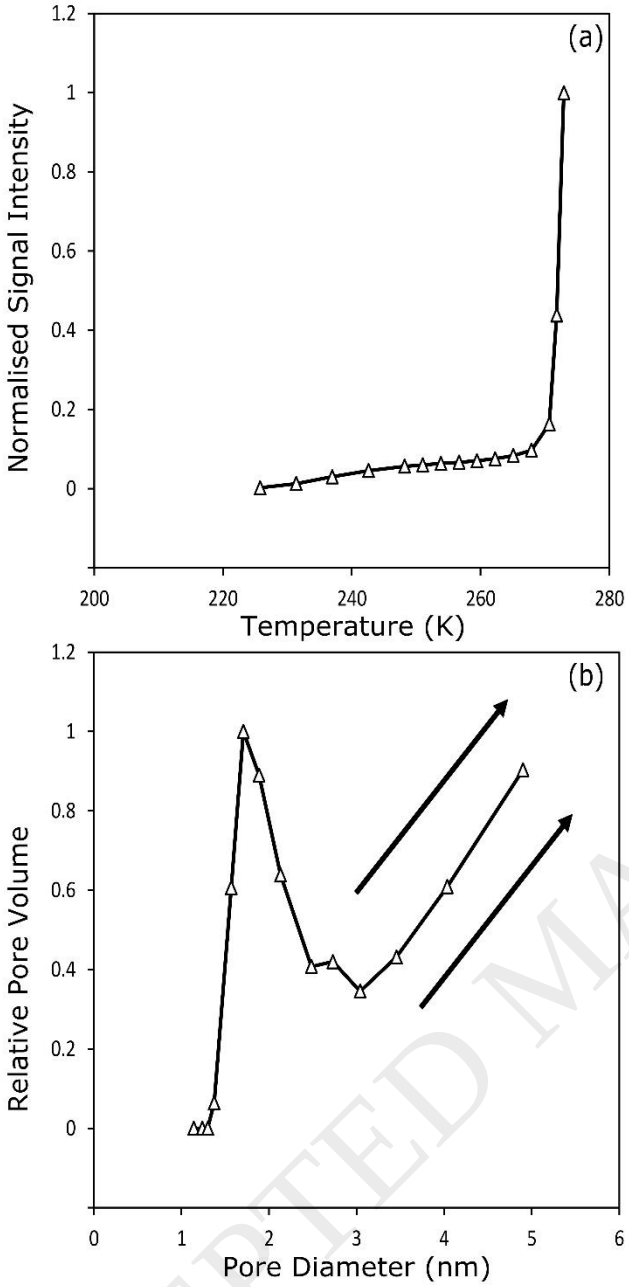

Figure 7. NMR melting curve for the macroreticular resin swollen with water and (b) the subsequent pore size distribution obtained using melting point depression parameters of k_c = 49.53 K nm and $2l$ = 0.53 nm.

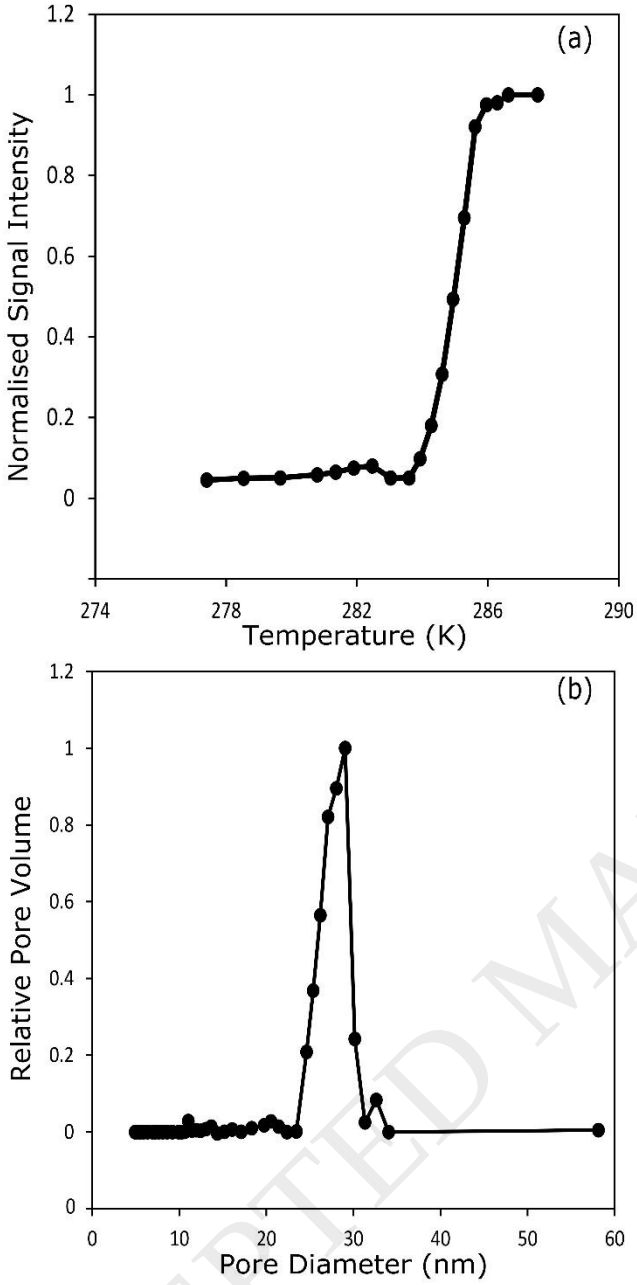

Figure 8. NMR melting curve for the macroreticular resin swollen with *t*-butanol and (b) the subsequent pore size distribution obtained using melting point depression parameters of k_c = 119.2 K nm and $2l$ = 1.7 nm.

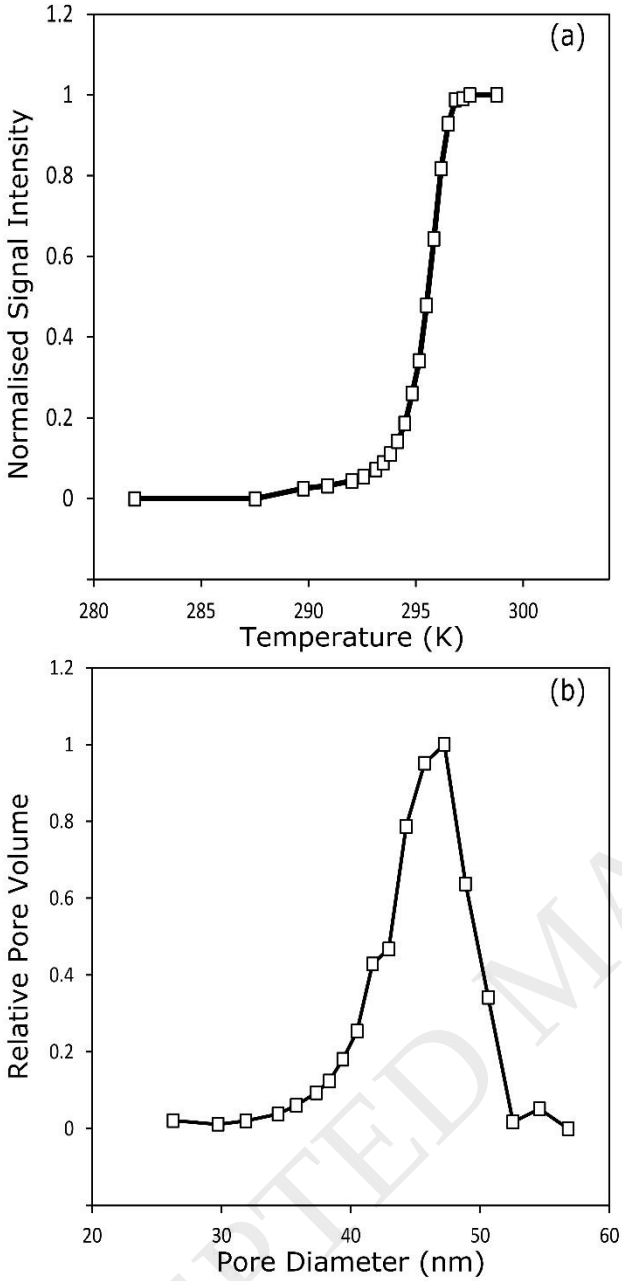

Figure 9. (a) NMR melting curve for the macroreticular resin swollen with menthol and (b) the subsequent pore size distribution obtained using melting point depression parameters of k_c = 219.3 K nm and $2l$ = 1.9 nm.